Applied Surface Science 256 (2010) 2453–2457

Contents lists available at ScienceDirect

Applied Surface Science

journal homepage: www.elsevier.com/locate/apsusc

Defects related room temperature ferromagnetism in p-type (Mn, Li) co-doped ZnO films deposited by reactive magnetron sputtering

C.W. Zou [a,b,*], H.J. Wang [a], M.L. Yi [a], M. Li [a], C.S. Liu [a], L.P. Guo [a], D.J. Fu [a], T.W. Kang [b]

[a] Accelerator Laboratory, Department of Physics and Key Laboratory of Acoustic Photonic Materials and Devices of Ministry of Education, Wuhan University, Wuhan 430072, China
[b] Quantum Functional Semiconductor Research Center, Dongguk University, Seoul 100-715, Republic of Korea

ARTICLE INFO

Article history:
Received 17 August 2009
Received in revised form 24 October 2009
Accepted 24 October 2009
Available online 1 November 2009

Keywords:
Ferromagnetism
Thin films
Reactive magnetron sputtering
ZnO

ABSTRACT

We report on the defects related room temperature ferromagnetic characteristics of $Zn_{0.95-x}Mn_xLi_{0.05}O$ (x = 0.01, 0.03, 0.05 and 0.08) thin films grown on glass substrates using reactive magnetron sputtering. By increasing the Mn content, the films exhibited increases in the c-axis lattice constant, fundamental band gap energy, coercive field and remanent magnetization. Comparison of the structural and magnetic properties of the as-deposited and annealed films indicates that the hole carriers, together with defects concentrations, play an important role in the ferromagnetic origin of Mn and Li co-doped ZnO thin films. The ferromagnetism in films can be described by bound magnetic polaron models with respect to defect-bound carriers.

1. Introduction

There has been much interest in magnetic semiconductors which exploit both the spin and the charge of the carriers, because the combination of the two degrees of freedom promises new functionality of memory, detector, and light emitting sources. Possible spintronic devices are spin-valve transistors, spin-light emitting diodes, and non-volatile storage and logic devices. A spin-polarized carrier population can be locally introduced by placing a ferromagnetic metal adjacent to a conventional semiconductor [1]. However, this approach results in only a small spin polarization [2]. An alternate approach is to form what is called diluted magnetic semiconductors (DMS), by substituting magnetic ions onto lattice sites of a semiconductor host [3]. Recently, it was suggested that a 100% spin-polarized carrier population might be achievable in appropriate systems [4]. The main challenge for practical application of the DMS materials is the attainment of a Curie temperature (T_c) at or above room temperature so as to be compatible with junction temperatures. Among the studies of transition metal (TM)-doped conventional III–V and II–VI semiconductors, TM-doped ZnO has become the most extensively studied set of materials following the prediction of Dietl et al. [5].

Theoretical calculations considering the ferromagnetic correlations mediated by holes originating from shallow acceptors in the ensemble of the localized spins predicted that ZnMnO materials (5 at.% Mn-doped p-type) would have a T_c above room temperature [5]. A recent theoretical work proposed that the ferromagnetic exchange could be mediated by shallow donor electrons that form bound magnetic polarons (BMP), which overlap to create a spin-split impurity band at the Fermi level [6]. However, the reported experimental results have been inconsistent and sometimes controversial [7–15]. Ferromagnetism was recently observed in insulating [16], n-type [17], and p-type ZnMnO [18]. Therefore, the origin of ferromagnetism in ZnMnO films has not yet been clearly elucidated and more research is needed to understand the underlying causes of the inconsistency. Despite the controversy and discrepancy reported in ZnMnO systems, more and more groups have observed high T_c ferromagnetism in p-type ZnMnO films and attributed the activation of ferromagnetism to the holes introduced by the doping of acceptors [8,19–21]. Li has been considered to be a promising acceptor impurity for making p-type ZnO by the first principles plane wave method [22] and Li-doped ZnO films have been successfully fabricated by various deposition methods such as simultaneous evaporation [23], metal organic chemical vapor deposition [24], and reactive magnetron sputtering [25]. As far as we know, there has been no report on the successful preparation of p-type ZnMnO by Li doping.

In this paper, we report the fabrication of p-type $Zn_{0.95-x}Mn_xLi_{0.05}O$ films by co-sputter of $Zn_{0.95}Li_{0.05}O$ ceramic and Mn

* Corresponding author. Tel.: +86 27 68753587; fax: +86 27 68753587.
E-mail address: Changweizou@hotmail.com (C.W. Zou).

0169-4332/$ – see front matter © 2009 Elsevier B.V. All rights reserved.
doi:10.1016/j.apsusc.2009.10.086

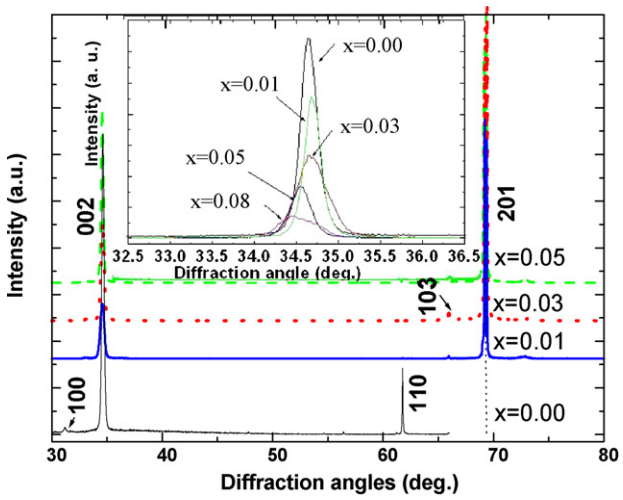

Fig. 1. XRD patterns for $Zn_{0.95-x}Mn_xLi_{0.05}O$ (x = 0.00, 0.01, 0.03, 0.05 and 0.08) thin films. *Inset*: Magnified pattern of the (0 0 2) diffraction peak.

metal targets and demonstrate defects and holes concentration-related bound magnetic polaron model for room temperature ferromagnetism.

2. Experimental details

The ceramic targets of $Zn_{0.95}Li_{0.05}O$ were synthesized by a solid reaction from starting materials ZnO (99.99%) and Li_2CO_3 (99.99%). The mixed powder was ball-milled for 24 h and preheated at 700 °C. Pellets were formed at 500 MPa pressure and sintered at 1050 °C for 3 h. The sputtering chamber was evacuated by a molecular pump to a base pressure below 1×10^{-4} Pa. An RF power of 150 W was used to sputter the $Zn_{0.95}Li_{0.05}O$ target. The DC power applied to the Mn target was set between 5 and 20 W for the $Zn_{0.95-x}Mn_xLi_{0.05}O$ (x = 0.01, 0.03, 0.05 and 0.08) films with different Mn concentrations. The targets were pre-sputtered for 5 min before the actual deposition in order to remove contamination from the target surface. During sputtering, the glass substrate temperature and substrate targets distance were set at 450 °C and 80 mm, respectively. Oxygen was introduced into the chamber as the reactive gas and the chamber pressure was fixed at 2×10^{-2} Pa. Rapid thermal annealing was carried out at temperatures of 400, 550, 700 °C for 30 s in a flowing oxygen atmosphere.

The films were structurally characterized in terms of X-ray diffraction (XRD, D8ADVANCE) and atomic force microscopy (AFM, SHIMADZUSPM-9500J3). An RM-1000 type Raman microspectrometer was used to clarify the local atomic arrangements of samples. The excitation source was an Ar^+ laser working at a wavelength of 514.53 nm. Chemical bonding states and chemical compositions of the films were analyzed by X-ray photoelectron spectroscopy (XPS). The absorption plot was obtained by a UV–vis–NIR spectrophotometer (VARIANCARY 5000). The magnetic measurement was carried out using a Quantum Design Superconducting Quantum Interference Device (SQUID) magnetometer. The field cooling (FC) and zero field cooling (ZFC) M–T curves were measured under magnetic field of 150 Oe.

3. Results and discussion

Fig. 1 shows the XRD θ–2θ scans for $Zn_{0.95-x}Mn_xLi_{0.05}O$ films doped with different Mn concentrations. All peak positions of the

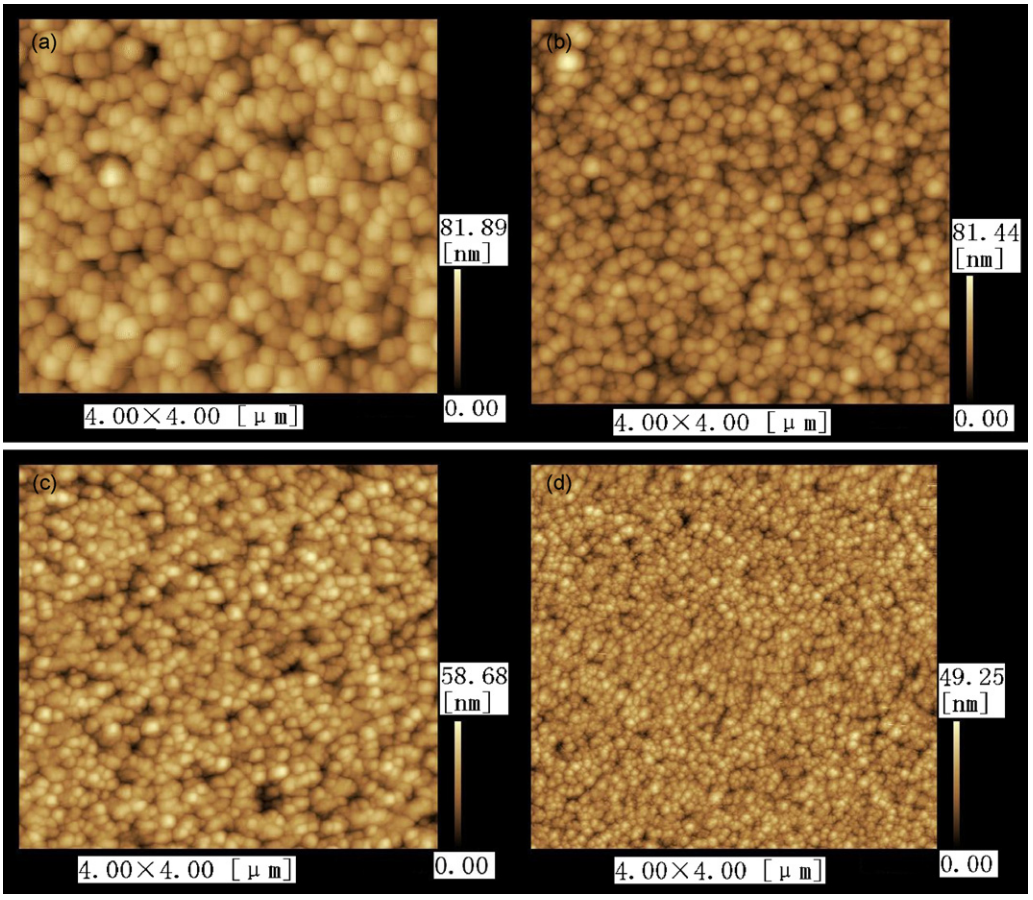

Fig. 2. AFM images for $Zn_{0.95-x}Mn_xLi_{0.05}O$ (x = 0.00, 0.01, 0.03, 0.05 and 0.08) thin films with different Mn concentrations.

films correspond to the standard diffraction pattern of wurtzite hexagonal ZnO. The absence of extra peaks in these XRD patterns suggests that the films are textured and also no precipitates or large-sized clusters are present in these films. Initially, a slight shift in the peaks to higher angles was observed at higher concentrations of Mn ions with x values of 0.01 and 0.03, which indicates a reduction in the lattice constant with Mn doping, which is expected as smaller Mn ions (for example, Mn^{2+} and Li^{+} ionic radii are 0.66 and 0.73 Å, respectively compared to 0.74 Å for Zn^{2+}) are incorporated into the Zn sites of the ZnO lattice. However, the XRD peaks shift to lower angles with further increase x values to 0.05 and 0.08. This can be attributed to interstitial ions or defects introduced by Mn doping. Also, XRD cannot detect really small size precipitates, especially if they are less than 5% in volume.

AFM measurements showed drastic changes in the roughness of the surface and grain size of the $Zn_{0.95-x}Mn_xLi_{0.05}O$ films with different Mn doping concentrations, as illustrated in Fig. 2. The reduction in the crystallite size with increasing Mn concentration agrees reasonably well with the estimates obtained from XRD data shown in Fig. 1. Similar result has been reported for ZnO films doped with Co by sol–gel method [26].

The chemical bonding states of the Mn 2p and Zn 2p in the $Zn_{0.90}Mn_{0.05}Li_{0.05}O$ and $Zn_{0.87}Mn_{0.08}Li_{0.05}O$ films were characterized by XPS measurement and shown in Fig. 3a and b, respectively. The XPS spectra have been charge corrected to the adventitious C 1 s peak at 284.2 eV. The binding energies of the Zn $2p_{3/2}$ and Mn $2p_{3/2}$ states for $Zn_{0.90}Mn_{0.05}Li_{0.05}O$ are located at 1021.9 and 640.6 eV, respectively. For the $Zn_{0.95}Mn_{0.05}O$ thin films, the binding energies of the Zn $2p_{3/2}$ and Mn $2p_{3/2}$ states located at 1021.7 and 640. 4 eV have been published previously [27]. The binding energies of Zn $2p_{3/2}$ and Mn $2p_{3/2}$ states for $Zn_{0.90}Mn_{0.05}Li_{0.05}O$ increased, compared to those of the $Zn_{0.95}Mn_{0.05}O$ film. Such an increase in binding energy results in a decrease of the iconicity of the Zn. Therefore the difference between the binding energies of the two samples can be ascribed to the presence of Li ions, that is, the Li atoms have substituted the Zn atoms in the lattice. From curve fitting, we find that there are two peaks at 640.5 and 641.4 eV attributed to Mn^{2+} and Mn^{3+}, respectively. Thus we may reach the conclusion that Mn-based binary and ternary oxide candidates have been produced on the surface of $Zn_{0.87}Mn_{0.08}Li_{0.05}O$ films.

Fig. 3c shows the Raman spectrum of the $Zn_{0.95-x}Mn_xLi_{0.05}O$ (x = 0.01, 0.03, 0.05, and 0.08) thin films with different Mn concentrations on Si (1 1 1) substrates. The strong Raman scattering peaks at 439 and 578 cm^{-1} are attributed to the non-polar optical phonon modes (E_2^{high}) and LO modes with A_1 symmetry (A_1(LO)), respectively [28]. According to group theory, the Raman active modes in ZnO are $A_1 + E_1 + 2E_2$ and [28], where A_1 and E_1 are polar and split into TO and LO phonons with different frequencies. The peak at 439 cm^{-1} is the high frequency E_2 mode characteristic of the wurtzite structure, while The A_1(LO) mode is known to be related to the defects such as oxygen vacancy, interstitial Zn in ZnO [29]. As a result, we think the appearance of A_1(LO) mode at 578 cm^{-1} can be attributed to interstitial ions or defects introduced by Mn doping. Similar results have been reported by implantation [30]. Therefore, the broadened of the A_1(LO) with increasing Mn concentrations indicating obvious degradation in crystallization and increase in defects concentration.

Optical absorption plots of the Mn-doped $Zn_{0.95}Li_{0.05}O$ thin films are shown in Fig. 3d, where the square of the transmitted intensity is plotted as a function of photon energy. The spectra clearly show that the band edge for all these films is in the range of 3.2–3.8 eV with band gap increasing for increasing Mn concentra-

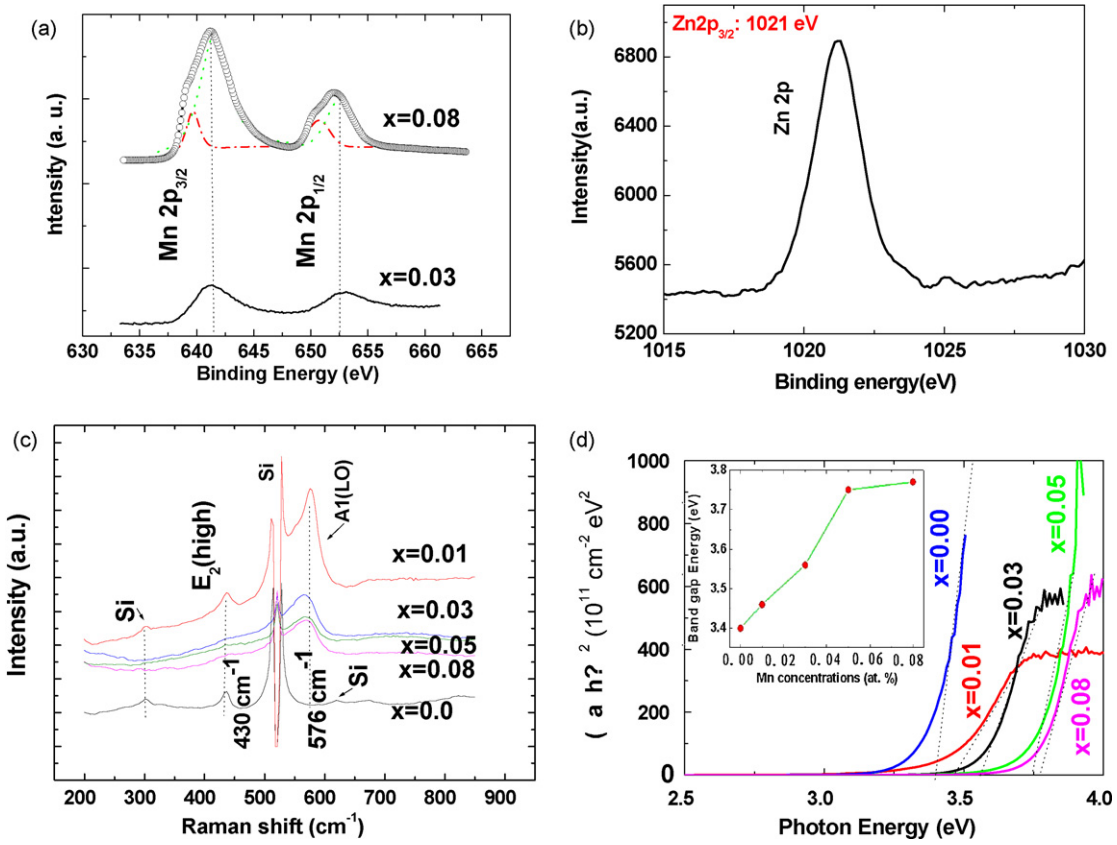

Fig. 3. XPS, Raman, and absorption plots for the (Mn, Li) co-doped ZnO films. (a) Mn 2p curves with x values of 0.03 and 0.08. (b) Zn 2p with x values of 0.05. (c) Raman spectrum. (d) Absorption plots.

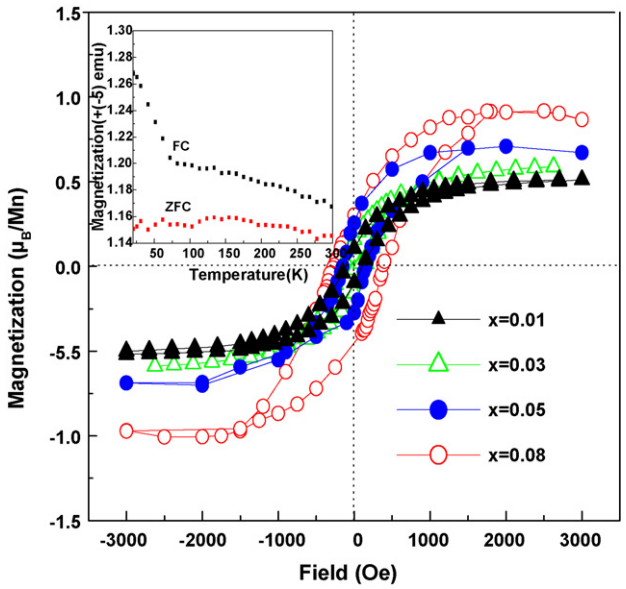

Fig. 4. Room temperature *M–H* and *M–T* curves for $Zn_{0.95-x}Mn_xLi_{0.05}O$ (x = 0.00, 0.01, 0.03, 0.05 and 0.08) thin films under a field of 1000 Oe parallel to the surface.

tion. This consistent change of band gap with an increase in Mn concentration suggests a uniform substitution of Mn for Zn ions in the lattice [31].

Magnetic measurements on $Zn_{0.95-x}Mn_xLi_{0.05}O$ films were performed in the temperature range of 5–300 K using a SQUID magnetometer. All the measurements were corrected for substrate effects. The result of magnetization as a function of applied field at 300 K is shown in Fig. 4. All the samples show ferromagnetic ordering at room temperature. The moment per Mn atom at 300 K increased with increasing Mn concentration. The sample with x values of 0.01 posses a net moment of 0.60μ_B/Mn atom, while sample with x values of 0.03 has a moment of 0.72μ_B/Mn atom, samples with x values of 0.05 has a moment of 0.76μ_B/Mn atom, and sample with x value of 0.08 has a moment of 0.8μ_B/Mn atom. The corresponding coercive fields (H_c) for above samples are 61, 39, 59, 80 Oe, respectively. The zero-field-cooled (ZFC) and field-cooled (FC) magnetization curves are on the $Zn_{0.90}Mn_{0.05}Li_{0.05}O$ film, which are kept separated up to 300 K which indicates that the T_c is well above room temperature. The peak on the ZFC curves at about 150 K shows the possibility of amorphous clusters existing.

Fig. 5 shows the room temperature magnetization versus field curves at room temperature for as-deposited and annealed

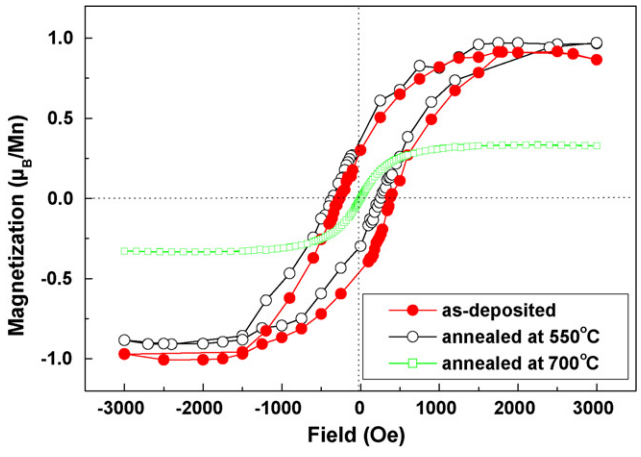

Fig. 5. Magnetization curves of the $Zn_{0.92}Mn_{0.03}Li_{0.05}O$ thin film annealed at various temperatures. *Inset*: Enlarged portion of the plot near origin.

$Zn_{0.90}Mn_{0.05}Li_{0.05}O$ films. The as-deposited film shows a saturation magnetization value (M_S) of over 0.8μ_B/Mn, whereas the annealed films show a decrease in trend with increasing annealed temperature. The carrier concentration is not much improved after annealing and is in the order of 10^{16} cm^{-3}, which suggests that FM does not depend upon the presence of a significant carrier concentration.

Resistivity and Hall effect measurements indicate that the presence of Li ions in ZnMnO decreases the resistivity by three orders from 10^3 Ωcm for $Zn_{0.95}Mn_{0.05}O$ to 18 Ωcm for $Zn_{0.90}Mn_{0.05}Li_{0.05}O$ films. The glass substrates used here can assure that the p-type conduction comes from the ZnO film rather than the substrate. The corresponding holes concentrations are 1.48×10^{16}, 2.36×10^{16}, 4.40×10^{16}, 3.62×10^{16} ions/cm^2 for the $Zn_{0.95-x}Mn_xLi_{0.05}O$ films with x values of 0.01, 0.03, 0.05, and 0.08, respectively. Although it is believed that the hole carriers are provided by the substitution of Li^+ ions for Zn^{2+} ions, the low hole concentration of holes concentration suggests that significant compensation of dopant and/or localization of holes occur in the (Mn, Li) co-doped ZnO films.

This relative high resistivity and low holes concentrations of the $Zn_{0.95-x}Mn_xLi_{0.05}O$ films unambiguously rule out the possible carrier mediated exchange, such as the Rudermann–Kittel–Kasuga–Yosida (RKKY) which is based on the exchange coupling between the magnetic ions and conduction band electrons. Moreover, conventional super exchange interactions cannot produce long-range magnetic order at concentrations of magnetic cation of only a few percent, i.e., 4 at.% Mn-doped ZnO [31].

Bound magnetic polarons model for oxide semiconductors as a function of doping and carrier density was predicted by Coey et al. [6]. The general formula for the oxide is $(A_{1-x}M_x)(O\square_\delta)_n$, where A is a non-magnetic cation, M is a magnetic cation, □ represents a donor defects, and the occurrence of different magnetic phases is determined by the polaron and cation percolation threshold δ_p and x_p, respectively. It is predicated that in oxide, ferromagnetism occurs when $\delta > \delta_p$ and $x < x_p$. The critical defect concentrations for (N□) establishing percolation threshold for long range ferromagnetism order can be estimated from $r^3(N\square/N_O)$, where N_O is the oxygen density for ZnO, and r is estimated to be about 3.8×10^{18} cm^{-3}. From the SQUID measurements shown in Fig. 4, it is observed that the M_S increases gradually with the increase in Mn concentrations, which is due to the larger defect density caused by Mn incorporation. For the as-deposited $Zn_{0.90}Mn_{0.05}Li_{0.05}O$ films, the calculated defect concentration is about 6×10^{17} cm^{-3}, whereas for the 700 °C annealed films, the value is calculated to be below 10^{16} cm^{-3}. The presence of such a large concentration of defects present in the as-deposited films allows for long-range FM in accordance with the BMP model. The coexistence of Mn^{3+} and Mn^{2+} may be also responsible for high Curie-temperature ferromagnetism via a double-exchange mechanism which couples magnetic ions in different charge states by virtual hopping of electron from one ion to other through interaction with p-orbital [32]. This fact has recently been reported by Garcia et al. [33] and compared with the fact regarding the La–Ca–Mn–O system in which ferromagnetism is also due to the coexistence of Mn^{4+} and Mn^{3+} [34]. Double-exchange has also been taken to explain the origin of room temperature magnetism in thin $(ZnO)_{1-x}(MnO_2)_x$ films and ZnO/MnO_2 multilayers [35].

We propose that ferromagnetic exchange here in $Zn_{0.95-x}Mn_xLi_{0.05}O$ films is mediated by shallow acceptor holes that form bound magnetic polarons, which overlap to create a spin-split impurity band one possibility of the high T_c (above room temperatures) may arise from the hybridization and charge transfer from the acceptor impurity band to 3d states of Mn ions near the Fermi level.

4. Conclusions

In summary, we have grown single crystalline $Zn_{0.95-x}Mn_xLi_{0.05}O$ thin films using reactive magnetron sputtering method. Room temperature ferromagnetism was observed in these films. XPS, XRD and optical measurements showed the presence of Mn ions in a tetrahedral crystal field and absence of any secondary phase or nano-clusters. Through depositing of the films with different Mn concentrations and annealing the films in oxidation atmospheres, it has been demonstrated that FM is not linked to conductivity and that defects plays a crucial role in mediating the FM in (Li, Mn) co-doped ZnO. These results explain why there is large variability in FM properties of films grown by conventional vapor-deposition method at high temperature since anion and cation defect concentrations depend strongly on temperature, growth pressure and growth rate, which are not easily reproduced from growth run to another. The absence of a correlation between the magnetism and conductivity support a bound polaron model for FM on (Mn, Li) co-doped p-type ZnO films.

Acknowledgments

This work was supported by National Natural Science Foundation of China under contract Nos.10435060 and 10675095 and by the Korea Science and Engineering Foundation through QSRC at Dongguk University.

References

[1] D.B. Buchholz, R.P.H. Chang, J.H. Song, J.B. Ketterson, Appl. Phys. Lett. 87 (2005) 082504.
[2] S.A. Wolf, D.D. Awschalom, R.A. Buhrman, J.M. Daughton, S. Von Molnar, M.L. Roukes, A.Y. Chtchelkanova, D.M. Treger, Science 294 (2000) 1488.
[3] J.K. Furdyna, J. Appl. Phys. 53 (1982) 7637.
[4] R.N. Gurzhi, A.N. Kalinenko, A.I. Kopeliovich, A.V. Yanousky, E.N. Bogachek, U. Landman, Phys. Rev. B 68 (2003) 125113.
[5] T. Dietl, H. Ohno, F. Matsukura, J. Cibert, D. Ferrand, Science 287 (2000) 1019.
[6] J.M.D. Coey, M. Venkatesan, C.B. Fitzgerald, Nat. Mater. 4 (2005) 173.
[7] K. Ueda, H. Tabata, T. Kawai, Appl. Phys. Lett. 79 (2001) 988.
[8] K.R. Kittilstved, N.S. Norberg, D.R. Gamelin, Phys. Rev. Lett. 94 (2005) 147209.
[9] K.R. Kittilstved, W.K. Liu, D.R. Gamelin, Nat. Mater. 5 (2006) 291.
[10] K.R. Kittilstved, D.A. Schwartz, A.C. Tuan, S.M. Heald, S.A. Chambers, D.R. Gamelin, Phys. Rev. Lett. 97 (2006) 037203.
[11] P. Sharma, A. Gupta, R.V. Rao, F.J. Owens, R. Sharma, R. Ahuja, J.M.O. Guillen, B. Johansson, G.A. Gehring, Nat. Mater. 2 (2003) 673.
[12] N. Khare, M.J. Kappers, M. Wei, M.G. Blamire, J.L.M.M. Driscoll, Adv. Mater. 18 (2006) 1449.
[13] X. Wang, J. Xu, B. Zhang, H. Yu, J. Wang, X. Zhang, J. Yu, Q. Li, Adv. Mater. 18 (2006) 2476.
[14] J.R. Neal, A.J. Behan, R.M. Ibrahim, H.J. Blythe, M. Ziese, A.M. Fox, G.A. Gehring, Phys. Rev. Lett. 96 (2006) 197208.
[15] O.D. Jayakumar, I.K. Gopalakrishnan, S.K. Kulshreshtha, Adv. Mater. 18 (2006) 1857.
[16] S.W. Jung, S.J. An, G.C. Yi, C.U. Jung, S.I. Lee, S. Cho, Appl. Phys. Lett. 80 (2002) 4561.
[17] D.P. Norton, S.J. Pearton, A.F. Hebard, N. Theodoropoulou, L.A. Boatner, R.G. Wilson, Appl. Phys. Lett. 82 (2003) 239.
[18] S.W. Lim, M.C. Jeong, M.H. Ham, J.M. Myoung, Jpn. J. Appl. Phys. 43 (2004) 280.
[19] H.Y. Xu, Y.C. Liu, C.S. Xu, Y.X. Liu, C.L. Shao, R. Mu, Appl. Phys. Lett. 88 (2006) 242502.
[20] Z.B. Gu, M.H. Lu, J. Wang, D. Wu, S.T. Zhang, X.K. Meng, Y.Y. Zhu, S.N. Zhu, Y.F. Chen, X.Q. Pan, Appl. Phys. Lett. 88 (2006) 082111.
[21] W.S. Yan, Z.H. Sun, Q. Liu, Z. Li, T. Shi, F. Wang, Z. Qi, G. Zhang, S. Wei, Appl. Phys. Lett. 90 (2007) 242509.
[22] X.Y. Duan, R.H. Yao, Y.J. Zhao, Appl. Phys. A 91 (2008) 467.
[23] K. Kobayashi, Y. Tomita, Y. Maeda, H. Haneda, Phys. Stat. Sol. 5 (2008) 3122.
[24] Y.J. Zeng, Z.Z. Ye, Y.F. Lu, J.G. Lu, W.Z. Xu, L.P. Zhu, B.H. Zhao, J. Phys. D Appl. Phys. 40 (2007) 1807.
[25] Y.J. Zeng, Z.Z. Ye, W.Z. Xu, L.L. Chen, D.Y. Li, L.P. Zhu, B.H. Zhao, Y.L. Hu, J. Cryst. Growth 283 (2005) 180.
[26] J. Hays, K.M. Reddy, N.Y. Graces, M.H. Engelhard, V. Shutthanandan, M. Luo, C. Xu, N.C. Giles, C. Wang, S. Thevuthasan, A. Punnoose, J. Phys. Condens. Matter 19 (2007) 266203.
[27] C.J. Cong, L. Liao, J.C. Li, L.X. Fan, K.L. Zhang, Nanotechnology 16 (2005) 981.
[28] C. Bundesmann, N. Ashkenov, M. Schubert, D. Spemann, T. Butz, E.M. Kaidashev, M. Lorenz, M. Grundmann, Appl. Phys. Lett. 83 (2003) 1974.
[29] K.A. Alim, V.A. Fonoberov, M. Shamsa, A.A. Balandin, J. Appl. Phys. 97 (2005) 124313.
[30] C.W. Zou, M. Li, H.J. Wang, M.L. Yin, C.S. Liu, L.P. Guo, D.J. Fu, T.W. Kang, Nucl. Instrum. Methods Phys. Res. Set. B 267 (2009) 1067.
[31] D. Chakraborti, J. Narayan, J.T. Prater, Appl. Phys. Lett 90 (2007) 062504.
[32] C. Liu, F. Yun, H. Morkoc, J. Mater. Sci. Mater. Electron. 16 (2005) 555.
[33] M.A. Garcia, M.L. Ruiz-Gonzalez, A. Quesada, J.L. Costa-Kramer, J.F. Fernandez, S.J. Khatib, A. Wennberg, A.C. Caballero, M.S. Martin-Gonzalez, M. Villegas, F. Briones, J.M. Gonzalez-Calbet, A. Hernando, Phys. Rev. Lett. 94 (2005) 217206.
[34] G.H. Jonker, J.H. Van Santen, Physica 16 (1950) 337.
[35] E.L. Ponce, A. Wennberg, M.S.M. Gonzalez, J.L.C. Kramer, M.A. Garcia, A. Quesada, A. Hernando, A.C. Caballero, M. Villegas, J.F. Fernandez, Jpn. J. Appl. Phys. 45 (2006) 7677.